



Late Pleistocene glacier dynamics of southwestern Montana and adjacent Idaho and paleoclimatic implications  
by Donald R Murray

A thesis submitted in partial fulfillment of the requirements for the degree of Master of Science in Earth Sciences  
Montana State University  
© Copyright by Donald R Murray (1989)

**Abstract:**

Application of glacial flow theory to reliable reconstructions of paleoglaciers allows calculation of the dynamics of these glaciers. Effective basal shear stresses calculated along the longitudinal profiles of these glaciers can be used to estimate the component of mass flux due to internal deformation. Assuming basal slip to be zero at the point where deformation mass flux is a maximum, minimum net accumulation and ablation gradients can be calculated. Using the continuity equation, minimum mass flux at the ELA can be estimated. Also, net winter accumulation can be calculated by dividing the mass flux at the ELA by the accumulation area. Because local climate, in part, controls the mass balance and dynamics of a glacier, this model provides information on the climatic setting of paleoglaciers.

The model also allows estimation of basal slip as a factor in point estimates of glacial flow. Application of the continuity equation above and below the ELA generates additional estimates of mass flux at discrete points along each glacier. The difference between calculated deformation mass flux and continuity flux at these points yields a first approximation of basal slip, which can be highly variable along the length of a glacier.

The model was developed on the late Pleistocene Big Timber glacier of west-central Montana and tested on five other paleoglaciers in the Northern Rocky Mountains of southwestern Montana and adjacent Idaho. Sensitivity analysis performed on Big Timber glacier shows that the results are accurate within 20%. Low ablation gradients, ranging from 1.9 to 5.4 mm/m for five of the six glaciers, suggest a cold, dry environment in this region during the late Pleistocene. Calculated average annual net accumulation for these glaciers is 20-75% below modern maximum snowpack values, indicating a drier climate during the full glacial period. Basal sliding accounts for most (> 90%) of the glacial flow near the terminus of each glacier, but is variable along the rest of the glacier. While the mass balance values are minima, they are assumed to be reasonable approximations of the actual values, unless very high basal slip rates occurred along the entire length of each glacier.

LATE PLEISTOCENE GLACIER DYNAMICS OF SOUTHWESTERN MONTANA AND  
ADJACENT IDAHO AND PALEOCLIMATIC IMPLICATIONS

by

Donald R. Murray

A thesis submitted in partial fulfillment  
of the requirements for the degree

of

Master of Science

in

Earth Sciences

MONTANA STATE UNIVERSITY  
Bozeman, Montana

December 1989

N398  
M9618

APPROVAL

of a thesis submitted by

Donald Richard Murray

This thesis has been read by each member of the thesis committee and has been found to be satisfactory regarding content, English usage, format, citations, bibliographic style, and consistency, and is ready for submission to the College of Graduate Studies.

December 20, 1989  
Date

William W. Locke III  
Chairperson, Graduate Committee

Approved for the Major Department

December 20 1989  
Date

Stephen G. L.  
Head, Major Department

Approved for the College of Graduate Studies

January 8, 1990  
Date

Henry L. Parsons  
Graduate Dean

## STATEMENT OF PERMISSION TO USE

In presenting this thesis in partial fulfillment of the requirements for a master's degree at Montana State University, I agree that the Library shall make it available to borrowers under rules of the Library. Brief quotations from this thesis are allowable without special permission, provided that accurate acknowledgement of source is made.

Permission for extensive quotation from or reproduction of this thesis may be granted by my major professor, or in his absence, by the Dean of Libraries when, in the opinion of either, the proposed use of the material is for scholarly purposes. Any copying or use of the material in this thesis for financial gain shall not be allowed without my written permission.

Signature

Donald R. Murray

Date

December 19, 1989

## ACKNOWLEDGEMENTS

The author wishes to thank the members of his committee, Dr. William W. Locke (Committee Chairman), Dr. Katherine Hansen-Bristow, and Dr. Joseph Ashley, for providing support, guidance and helpful criticism throughout the project. Dr. Locke first suggested the topic and was extremely helpful in nurturing the project as it developed. Thanks are also due to Dr. James McCalpin of Utah State University for use of his unpublished work on glacier dynamics of the Sangre de Cristo Range and for discussion of the methods used in this project. I also wish to thank the Department of Earth Sciences for accepting me into the graduate program and for providing a productive and amiable atmosphere in which to work; my parents, William and Barbara Murray, for encouraging me to do whatever makes me happy; my wife, Diana Shellenberger, for field assistance, copyediting and moral support; and finally Bud Ebbett of Lyndon State College for providing the initial spark of my interest in glaciers and geology. This project was partially funded by GSA Research Grant 4051-88 and the D.L. Smith Scholarship through the Department of Earth Sciences.

## TABLE OF CONTENTS

	Page
INTRODUCTION . . . . .	1
The Problem . . . . .	1
Previous Work . . . . .	3
Theoretical Considerations . . . . .	4
Glacier Dynamics . . . . .	4
Equilibrium Line Altitude (ELA) . . . . .	4
Glacier Flow Velocities . . . . .	5
Mass Balance Gradients . . . . .	8
The Study Area . . . . .	11
Regional Setting . . . . .	11
Geology . . . . .	14
Present Climate . . . . .	14
Late-Pleistocene Climate . . . . .	19
METHODS . . . . .	21
Valley Selection . . . . .	23
Glacier Geometry . . . . .	24
Basal Shear Stresses . . . . .	29
Location of the ELA . . . . .	33
Lateral Moraines . . . . .	33
Lowest Cirque Elevation . . . . .	34
Toe-Headwall Altitude Ratio (THAR) . . . . .	34
Accumulation-Area Ratios (AAR) . . . . .	35
Estimated ELAs . . . . .	35
Glacier Flow . . . . .	36
Ice Deformation . . . . .	36
Basal Slip . . . . .	37
Average Velocity . . . . .	39
Ablation/Accumulation Gradients . . . . .	40
Paleoclimatic Interpretation . . . . .	44
RESULTS . . . . .	48
Case Study - Big Timber Canyon . . . . .	48
Valley Selection . . . . .	48
Glacier Geometry . . . . .	48
Basal Shear Stresses . . . . .	53
Location of the ELA . . . . .	56
Lateral Moraines . . . . .	57
Lowest Cirque Elevation . . . . .	57
Toe-Headwall Altitude Ratio (THAR) . . . . .	57

TABLE OF CONTENTS -- continued

	Page
Accumulation Area Ratio (AAR) . . . . .	57
Final ELA . . . . .	58
Glacier Flow . . . . .	59
Ablation/Accumulation Gradients . . . . .	59
Sensitivity and Error Analysis . . . . .	63
Results from other Valleys . . . . .	68
Lemhi Range . . . . .	68
Stroud Creek Glacier . . . . .	69
Everson Creek Glacier . . . . .	73
Mill Creek Glacier . . . . .	76
Meadow Lake Glacier . . . . .	80
Beaverhead Range . . . . .	83
Miner Lakes Glacier . . . . .	84
Summary . . . . .	89
DISCUSSION . . . . .	90
The Model . . . . .	90
Glacier Reconstruction . . . . .	90
Basal Shear Stresses . . . . .	93
Glacier Velocity - Ice Deformation . . . . .	95
Glacier Velocity - Basal Slip . . . . .	97
Field Observations . . . . .	98
Other Methods . . . . .	99
This study . . . . .	101
Mass Balance . . . . .	102
The Results . . . . .	103
Stroud Creek versus Everson Creek . . . . .	103
Comparison to Mill Creek . . . . .	104
Comparison of all valleys . . . . .	107
Basal Slip . . . . .	108
Paleoclimatic Interpretations . . . . .	110
Mass balance gradients . . . . .	110
This study . . . . .	111
Other studies . . . . .	113
Net Accumulation . . . . .	113
Comparison to other studies . . . . .	115
CONCLUSIONS . . . . .	118
Suggestions for Future Study . . . . .	120
Dynamics Modeling . . . . .	120
Paleoclimatic Modeling . . . . .	121
REFERENCES CITED . . . . .	123

TABLE OF CONTENTS -- continued

	Page
APPENDICES . . . . .	129
Appendix A - Topographic maps and air photos . . . . .	130
Appendix B - Program for calculating theoretical glacier profiles . . . . .	132
Appendix C - Program for calculating shear stress . . . . .	138
Appendix D - Program for calculating ablation gradients . . . . .	144
Appendix E - Program for calculating accumulation gradients . . . . .	147
Appendix F - Data for Stroud Creek . . . . .	150
Appendix G - Data for Everson Creek . . . . .	152
Appendix H - Data for Mill Creek . . . . .	154
Appendix I - Data for Meadow Lake . . . . .	156
Appendix J - Data for Miner Lakes . . . . .	158



## LIST OF TABLES

Table	Page
1. Analysis of the number of existing lateral moraines in a valley, given differences in climate between two successive glaciations . . . . .	27
2. Big Timber paleoglacier morphology and rheology . . . . .	54
3. ELA estimates for Big Timber glacier . . . . .	56
4. Average annual net ablation on Big Timber glacier . . . . .	61
5. Mass balance and basal slip results for Big Timber glacier . . . . .	64
6. Error and probability analysis of map-induced errors . . . . .	66
7. Mass balance and basal slip results for Stroud Creek glacier . . . . .	72
8. Mass balance and basal slip results for Everson Creek glacier . . . . .	75
9. Mass balance and basal slip results for Mill Creek glacier . . . . .	80
10. Mass balance and basal slip results for Meadow Lake glacier . . . . .	84
11. Mass balance and basal slip results for Miner Lakes glacier . . . . .	88
12. Values of the flow law constant A . . . . .	96
13. Mass balance estimates for Stroud Creek glacier assuming 0, 10, 20 and 50% basal slip . . . . .	106
14. Mass balance summary for all the glaciers . . . . .	107
15. Net accumulation . . . . .	114
16. Topographic maps and aerial photographs used for glacier reconstruction . . . . .	131

LIST OF TABLES -- continued

Table	Page
17. Stroud Creek paleoglacier morphology and rheology . . . .	151
18. Everson Creek paleoglacier morphology and rheology . . . .	153
19. Mill Creek paleoglacier morphology and rheology . . . . .	155
20. Meadow Lake paleoglacier morphology and rheology . . . . .	157
21. Miner Lakes paleoglacier morphology and rheology . . . . .	159

## LIST OF FIGURES

Figure	Page
1. General relationships between climate, glacier response and geologic evidence . . . . .	2
2. Mass exchange on a steady state glacier . . . . .	5
3. Components of glacier flow . . . . .	6
4. Generalized mass balance gradients for maritime and continental glaciers . . . . .	9
5. Location and physiography of the study area . . . . .	12
6. General areas of western Montana and adjacent Idaho covered by ice during the last glacial maximum . . . . .	13
7. Streamlines of mean January surface winds over the western United States . . . . .	15
8. Climographs and locations of selected cities within the study area . . . . .	16
9. Modern snow accumulation gradients . . . . .	18
10. Flowchart of the methodology . . . . .	22
11. Comparison of the shapes of maritime and continental glaciers . . . . .	26
12. Comparison of the difference in elevation between the ice centerline and the ice margins on modern glaciers . . . . .	28
13. Values of the shape factor (F) for varying parabolic glacier cross-sections . . . . .	31
14. Variables used in calculating theoretical glacier profiles . . . . .	32
15. Mass balance of the Yellowstone ice cap . . . . .	41
16. Continuity theory . . . . .	43
17. Photo of Big Timber Canyon . . . . .	49

LIST OF FIGURES -- continued

Figure	Page
18. Map of Big Timber Canyon and the glacier reconstruction . . . . .	50
19. Longitudinal profile of Big Timber glacier . . . . .	52
20. Average basal shear stress along Big Timber glacier . . . . .	55
21. Hypsometric curve of Big Timber glacier used to estimate ELA using AAR method . . . . .	58
22. Mass flux on Big Timber glacier . . . . .	60
23. Mass balance of Big Timber glacier . . . . .	62
24. Map of Stroud and Everson creek valleys and the glacier reconstructions . . . . .	70
25. Longitudinal profile of Stroud Creek glacier . . . . .	71
26. Longitudinal profile of Everson Creek glacier . . . . .	74
27. Map of Mill Creek valley and the glacier reconstruction . . . . .	77
28. Longitudinal profile of Mill Creek glacier . . . . .	79
29. Map of Meadow Lake Canyon and the glacier reconstruction . . . . .	81
30. Longitudinal profile of Meadow Lake glacier . . . . .	82
31. Map of Miner Lakes valley and the glacier reconstruction . . . . .	86
32. Longitudinal profile of Miner Lakes glacier . . . . .	87
33. An attempt to model mass balance gradients using mass flux and area . . . . .	100
34. Comparison of calculated net accumulation to modern snowpack accumulation gradients . . . . .	116
35. FORTRAN program for calculating theoretical glacier profiles . . . . .	133

LIST OF FIGURES -- continued

Figure	Page
36. FORTRAN program for calculating average effective basal shear stress . . . . .	139
37. BASIC program for calculating ablation gradients . . . . .	145
38. BASIC program for calculating accumulation gradients . . . . .	148

## ABSTRACT

Application of glacial flow theory to reliable reconstructions of paleoglaciers allows calculation of the dynamics of these glaciers. Effective basal shear stresses calculated along the longitudinal profiles of these glaciers can be used to estimate the component of mass flux due to internal deformation. Assuming basal slip to be zero at the point where deformation mass flux is a maximum, minimum net accumulation and ablation gradients can be calculated. Using the continuity equation, minimum mass flux at the ELA can be estimated. Also, net winter accumulation can be calculated by dividing the mass flux at the ELA by the accumulation area. Because local climate, in part, controls the mass balance and dynamics of a glacier, this model provides information on the climatic setting of paleoglaciers.

The model also allows estimation of basal slip as a factor in point estimates of glacial flow. Application of the continuity equation above and below the ELA generates additional estimates of mass flux at discrete points along each glacier. The difference between calculated deformation mass flux and continuity flux at these points yields a first approximation of basal slip, which can be highly variable along the length of a glacier.

The model was developed on the late Pleistocene Big Timber glacier of west-central Montana and tested on five other paleoglaciers in the Northern Rocky Mountains of southwestern Montana and adjacent Idaho. Sensitivity analysis performed on Big Timber glacier shows that the results are accurate within 20%. Low ablation gradients, ranging from 1.9 to 5.4 mm/m for five of the six glaciers, suggest a cold, dry environment in this region during the late Pleistocene. Calculated average annual net accumulation for these glaciers is 20-75% below modern maximum snowpack values, indicating a drier climate during the full glacial period. Basal sliding accounts for most (> 90%) of the glacial flow near the terminus of each glacier, but is variable along the rest of the glacier. While the mass balance values are minima, they are assumed to be reasonable approximations of the actual values, unless very high basal slip rates occurred along the entire length of each glacier.

## INTRODUCTION

### The Problem

There is an intimate relationship between climate and glaciation (Fig. 1), such that the dynamics (thickness, rate of flow and length) of a glacier are controlled to a large extent by changes in climate (Meier, 1965; Andrews, 1975). Climatic changes during the late Pleistocene (79,000 to 10,000 years ago) have been characterized by several global glacial advances and retreats. Evidence that late Pleistocene glaciers existed in some valleys of the Northern Rocky Mountains, which do not have glaciers at present, suggests that the paleoclimate must have been different from the present. The existence of glaciers does not, however, provide an actual measure of temperature or precipitation, but certain features of glaciers may be used as proxies to these climatic variables. Because the dynamics of a glacier are controlled in part by climate, reconstructed dynamics of paleoglaciers can be used as proxies to climate. In this study, a model is developed to interpret the ice dynamics of paleoglaciers. Although this project concentrates on the development of the model, the application of this model to six paleoglaciers that existed in southwestern Montana and adjacent Idaho during the last glacial maximum (20,000 years ago) suggests the magnitude and direction of late Quaternary changes in precipitation.

Changes in climate affect the mass balance of a glacier, which is a measure of the balance between mass gain (accumulation) and mass loss (ablation) on a glacier. On alpine glaciers, accumulation occurs mainly as snowfall while ablation takes place mainly through melt (Sugden and John, 1976). Changes in mass balance cause a dynamic response in the glacier. An increase in thickness generally causes an increase in the velocity and mass flux, which cause the glacier to advance (Nye, 1960; Meier, 1965). Thus, mass flux is an indicator of the mass balance of the glacier. For an ideal steady state glacier (one that is neither advancing or retreating), net accumulation is equal to net ablation (gain = loss). The calculated mass balance (i.e. net accumulation) of a steady state paleoglacier could be used as a crude proxy indicator of the paleoprecipitation on that glacier.

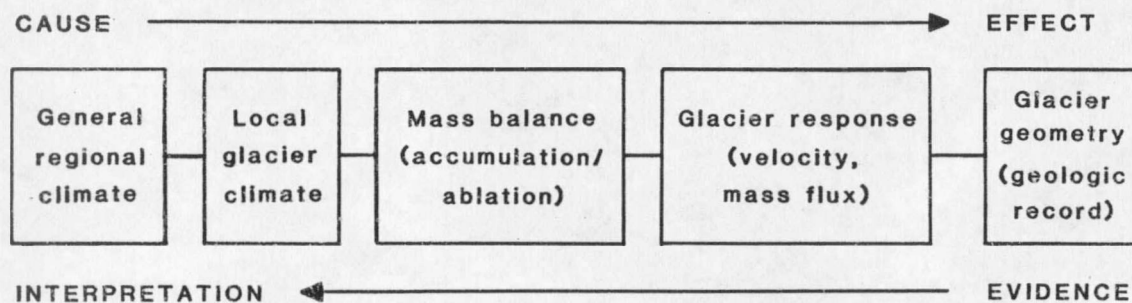


Figure 1. General relationships between climate, glacier response and geologic evidence of an individual glacier (left to right) (after Meier, 1965; Andrews, 1975). This study uses the reverse approach by interpreting mass balance and climate from the geologic record.

Working backwards through the pattern of study usually applied to climate-glacier relationships (Fig. 1), it is feasible to calculate the mass balance of paleoglaciers if the dynamics of these glaciers can be reconstructed (Haeberli and Penz, 1985; McCalpin, 1986). In



the Northern Rocky Mountains, many alpine paleoglaciers left clear evidence of their maximum areal extent in the form of moraines and trimlines. This evidence allows reconstruction of the former glacier shape and thickness. Ice velocity and mass flux can be estimated by applying ice flow theory to the reconstructed paleoglacier geometry. Mass flux through the equilibrium-line altitude of the paleoglacier provides an estimate of mass balance (net accumulation and net ablation). As a result, reconstruction of paleoglacier dynamics can be used to provide an approximation of paleoprecipitation (accumulation) on the glacier.

#### Previous Work

Only a few studies have used glacial mass balance as inferred from the ice dynamics of paleoglaciers to model paleoclimate. Haeberli and Penz (1985) applied this method to late Pleistocene paleoglaciers in the Alps. Although their methods allowed for only low precision, their estimates showed the Alps to be cold and dry during the last glacial maximum. McCalpin (1986) examined the ice flow dynamics and mass balances of paleoglaciers in the Sangre de Cristo Mountains of south-central Colorado and found that the calculated balances depended greatly on the flow regimes (extending, compressing, or uniform) of the glaciers. Using his method, only balances calculated in uniform flow regimes could be considered valid. Leonard and others (1986) used a similar method to model the climate of the Colorado Front Range during the late Pleistocene. Their

results show that area to be much drier during the glacial maximum than was previously thought.

In each of these ice dynamics studies, the method was applied to all the valleys within each study area. In some cases, irregularities in the geometries of the paleoglaciers (icefalls, stepped valleys) would have produced either overestimates or underestimates of mass balance (McCalpin, 1986). It is suggested that when using ice flow theory to model paleoglaciers, restrictions should be placed on the valley selection (applying the valleys to the method rather than the method to the valleys), thereby ensuring the quality of the results.

### Theoretical Considerations

#### Glacier Dynamics

The geometry of a glacier is a response to the flow behavior of ice over the underlying topography. As such, if the geometry of the glacier is known, ice flow laws can be applied to this geometry to calculate values of velocity and mass flux (Nye, 1952; Paterson, 1981).

Equilibrium-Line Altitude (ELA). The equilibrium-line altitude (ELA) is an important descriptor of any glacial system because it is the line where mass balance changes from net accumulation to net ablation. On a steady state glacier (Fig. 2), the net accumulation, the net ablation, and the mass flux (velocity x cross-sectional area) through the ELA are all equal over a given period of time (Andrews, 1975). In this steady state system, net mass balance is zero. The mass flux through the ELA is somewhat less than the total mass

exchange (where total accumulation = total ablation) on the glacier because there is seasonal accumulation below the ELA and seasonal ablation above the ELA. However, the mass flux at the ELA is equal to the net mass exchange, and balances the net accumulation above the ELA and the net ablation below the ELA. Once the ELA of a paleoglacier is located, the net mass exchange (therefore net accumulation and net ablation) can be determined by calculating the glacier velocity and multiplying it by the cross-sectional area at the ELA.

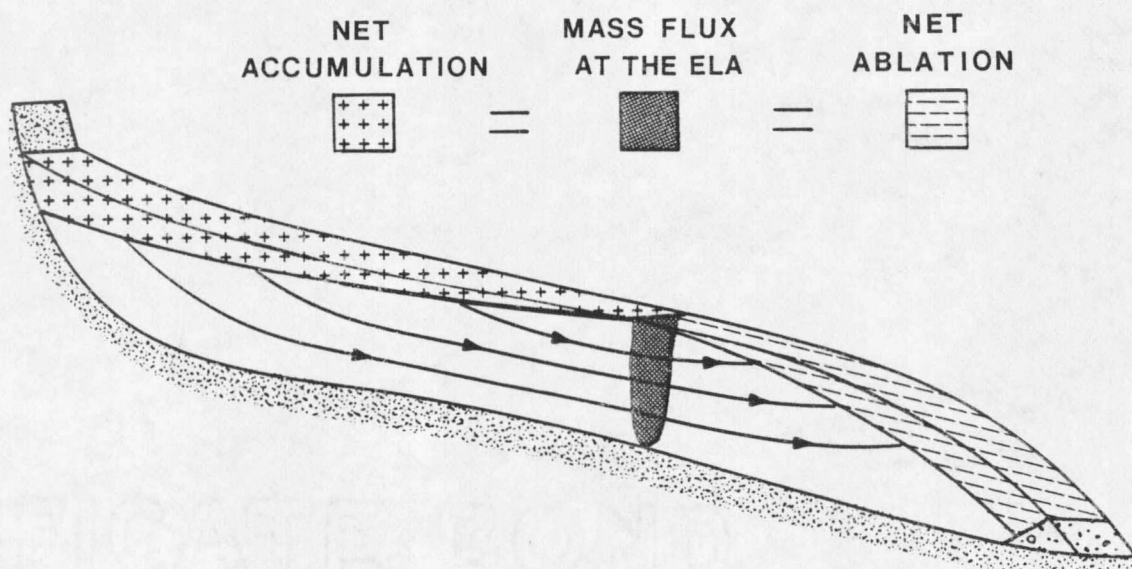


Figure 2. Mass exchange on a steady state glacier where net accumulation, net ablation and mass flux at the ELA are all equal.

Glacier Flow Velocities. Glacier movement can be broken down into components of ice deformation and basal sliding (Fig. 3). When ice is under pressure (stress), deformation takes place along internal planes of ice crystals. From laboratory experiments, Glen (1952) showed that the relationship of the strain rate (rate of deformation)

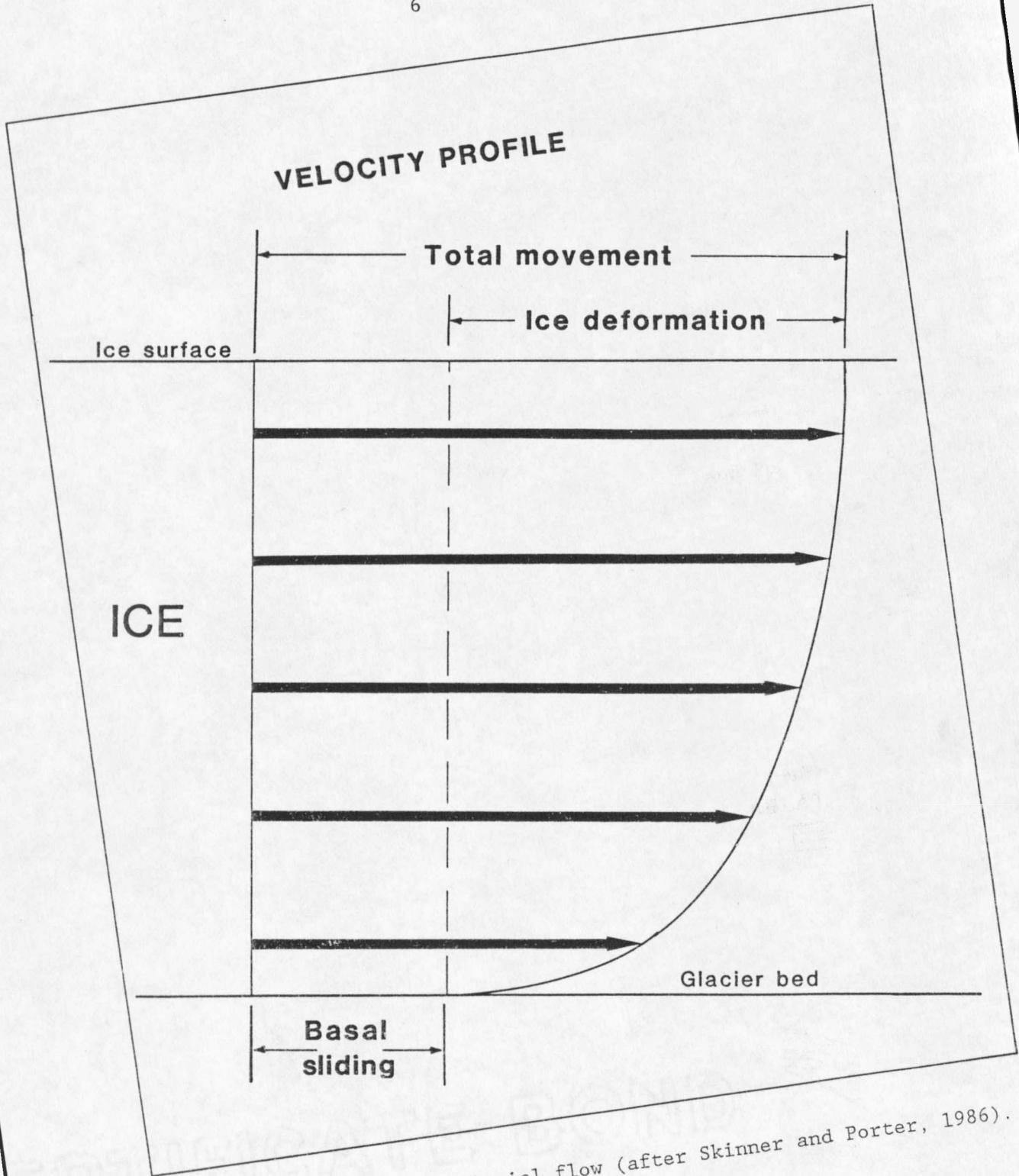


Figure 3. Components of glacial flow (after Skinner and Porter, 1986).

( $\dot{\epsilon}$ ) to shear stress ( $\tau$ ) could be expressed as:

$$\dot{\epsilon} = A \tau^n \quad (1)$$

where A is a temperature dependent constant and n is the slope of the strain rate curve. This is referred to as Glen's flow law. Laboratory and field experiments have shown that a value of  $n = 3$  is appropriate for glaciers (Paterson, 1981). Shear stress is a function of the glacier thickness and surface slope and has been found to vary from about 0.5 to 1.5 bars for modern glaciers (Nye, 1952). Estimates of the basal shear stresses of paleoglaciers (Mathews, 1967; Pierce, 1979) have indicated that this range is also valid for former glaciers. By integrating the strain rate function over small increments of glacial thickness (Nye, 1952; Paterson, 1981), the velocity at the centerline due to ice deformation can be determined (see Methods). Using this integral, deformation velocity varies as the fourth power of the glacier thickness so accurate estimation of thickness is needed. While Glen's flow law provides a method of determining the deformation velocity, this velocity is only part of the total flow through a cross-section.

The other component of glacial flow through a cross-section occurs from the glacier sliding over its bed (Fig. 3). Sliding velocities in modern glaciers have been directly observed in boreholes or have been determined by subtracting the calculated velocity due to deformation from the observed surface velocity (Paterson, 1981). The amount of basal sliding (basal slip) has been measured to account for 3-90% of total velocity on modern glaciers (Andrews, 1975; Paterson, 1981). Several models have been developed (summarized in Weertman,

1979; Raymond, 1980; Paterson, 1981) to explain basal slip, but there has been little agreement between observations and theory. For paleoglaciers, actual surface velocity cannot be compared with calculated deformation (creep) velocity, therefore, estimation of basal slip on these glaciers presents a problem.

Studies using ice dynamics to model mass balance (Haeberli and Penz, 1985; Leonard and others, 1986; McCalpin, 1986, Holmlund, 1988) usually assumed a constant basal slip, yet this did not consider the fact that slip can vary along the length of the glacier. Holmlund (1988) used an average value of 50% slip to calculate the mass balance on the modern Storglaciaren in Sweden, but actual measurements showed that basal slip locally accounted for 80-90% of the motion. Because slip varies along the length of a glacier, local calculations of slip must be made for an accurate assessment of the local flow regime.

Mass Balance Gradients. Mass balance provides a key to the activity (velocity, mass flux) of a glacier. Accumulation and ablation gradients show the relationship of net accumulation and net ablation, respectively, to elevation (Fig. 4), and as such, provide a measure of a glacier's activity (Andrews, 1975). These gradients are expressed in terms of change of net thickness (mm) of water accumulated or melted with elevation (m) above or below the ELA (thus mm/m).

Both ablation and accumulation tend to change linearly with elevation, therefore average gradients are reasonable descriptors (Andrews, 1975). High ablation gradients ( $> 10$  mm/m) are typical of glaciers in maritime environments where glacier activity is great due

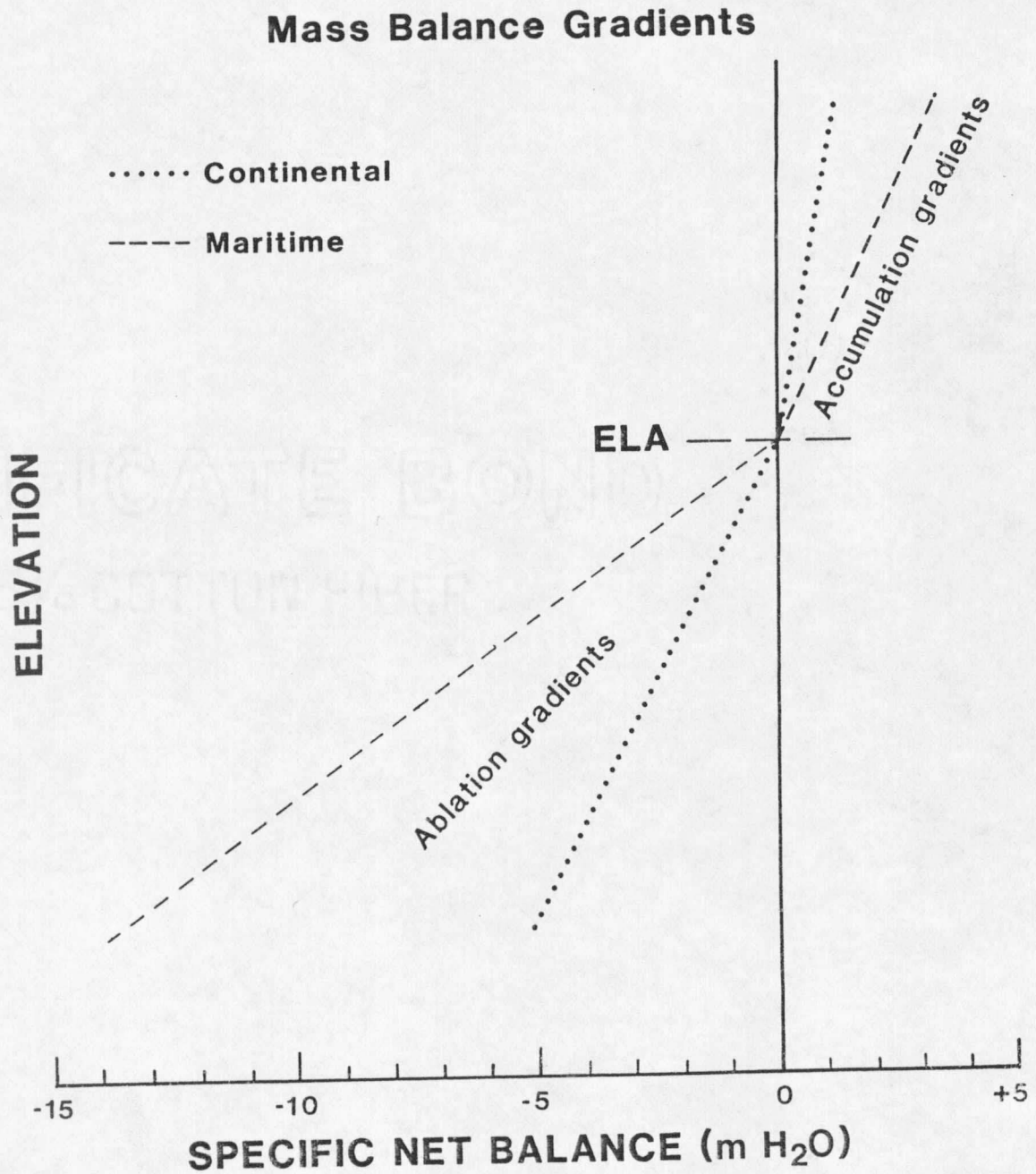


Figure 4. Generalized mass balance gradients for maritime and continental glaciers.

to the increased accumulation. Ablation gradients decrease inland toward more continental environments, to values of 2-7 mm/m (Fig. 4) (Meier and others, 1971; Andrews, 1975). Ablation gradients also decrease in value from temperate to polar climates. An exception to this trend is the occurrence of high gradients on small cirque glaciers in the Rocky Mountains of Wyoming and Montana. This exception can be accounted for by the local microclimates of small niche glaciers like these that produce large amounts of snow accumulation from wind drifting and orographic precipitation (Meier and others, 1971). On moderate sized glaciers, however, ablation gradients should be more indicative of regional climate (Meier and others, 1971; Andrews, 1975).

On modern glaciers, mass balance is directly measured on the glacier surface or can be determined using photogrammetric, hydrologic, or reconnaissance methods (Paterson, 1981). Balance gradients are determined using the measured mass balance and the areal distribution of the glacier with elevation. On paleoglaciers, these methods cannot be employed because the glacier no longer exists. However, if net accumulation and net ablation can be estimated by calculating net mass exchange at the ELA using reconstructed ice dynamics, average net balance gradients can then be determined. These gradients can be used to determine the annual net accumulation or ablation above or below a point on the glacier. The gradients can also be used as proxies to climate by comparison with modern analogs.



The Study AreaRegional Setting

The mountains of southwestern Montana and adjacent Idaho (Fig. 5) show extensive evidence of late Pleistocene glaciation (Alden, 1953; Porter and others, 1983). The large number of glaciated valleys provides an opportunity to select only those valleys that comply with the criteria in the model, including valleys with well defined glacial features and constant or slowly varying gradients (see Methods). The study area consists generally of northwest-southeast trending mountain ranges separated by broad valleys. The region is bounded on the east by the flat terrain of the Great Plains and on the west by the Salmon River Mountains of central Idaho. The relatively low, flat area of the Snake River Plain lies to the south. During the late Pleistocene, the region was bounded to the north by the Laurentide and Cordilleran ice sheets (Porter and others, 1983) and to the southeast by the Yellowstone ice cap (Pierce, 1979) (Fig. 6). The presence of these ice sheets significantly altered the regional topography during the last glacial maximum.

Six valleys (Fig. 6) were used to model paleoglacier dynamics and the paleoenvironment in this area. Big Timber Canyon (#1) in the Crazy Mountains was used to develop and refine the model. Four valleys (#3-6; Mill Creek, Stroud Creek, Everson Creek, and Meadow Lake) in the Lemhi Range were selected to test the local variability of the model. One other valley (#2; Miner Lakes) in the Beaverhead Range was also studied to test the regional applicability of the

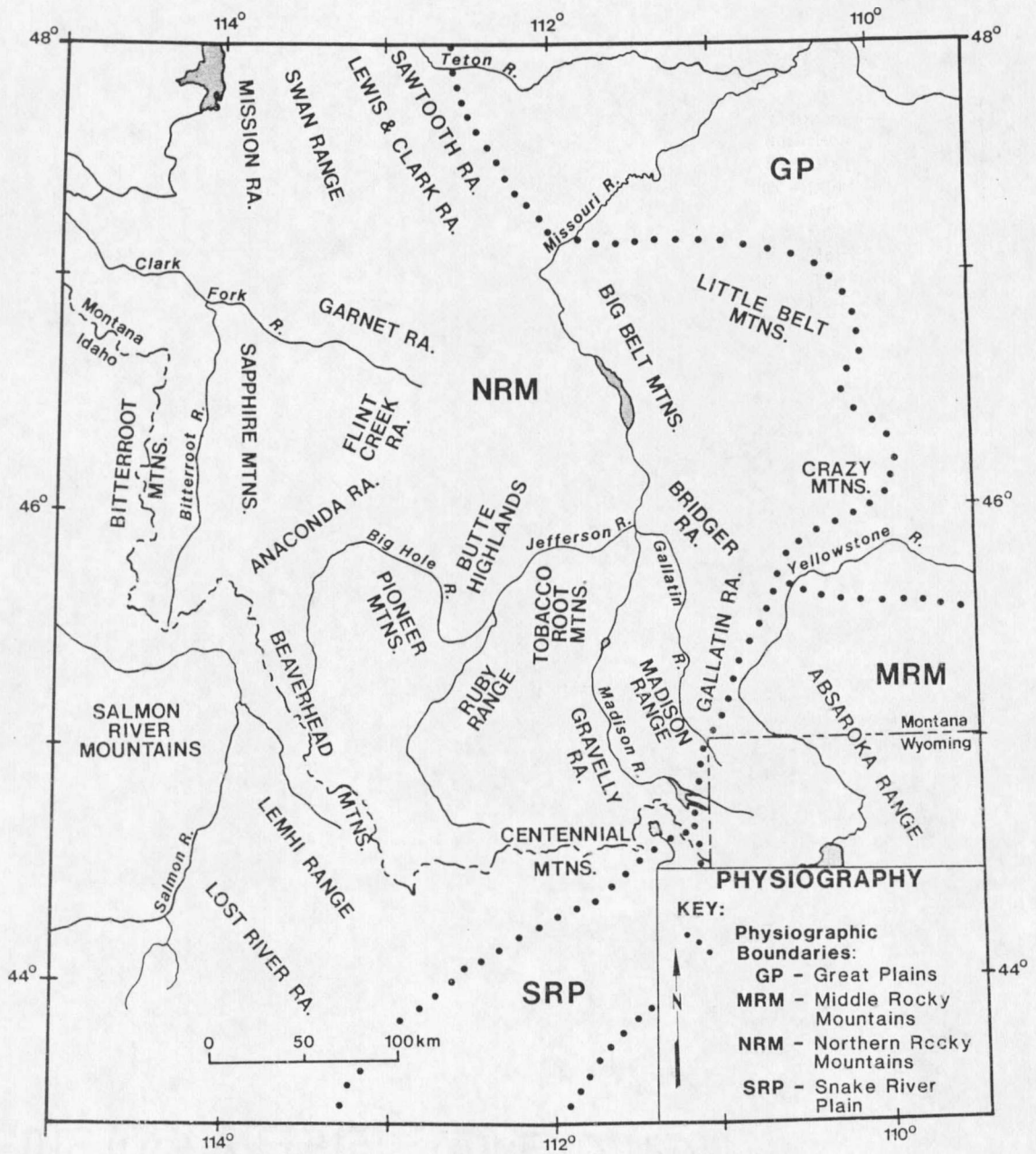


Figure 5. Location and physiography of the study area.

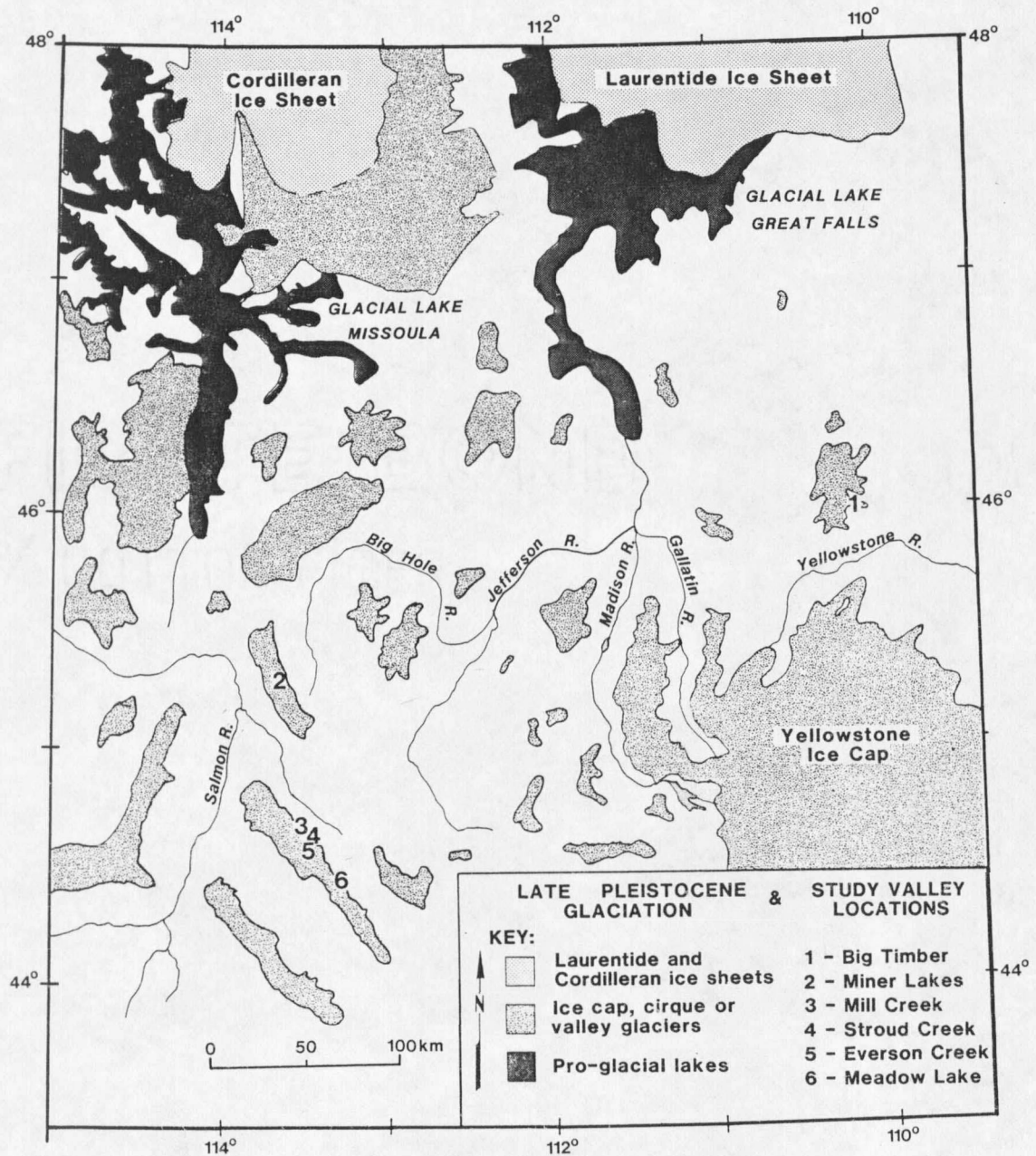


Figure 6. General areas of western Montana and adjacent Idaho covered by ice during the last glacial maximum (Taylor and Ashley, 1986; Waitt and Thorson, 1983; Fullerton and Colton, 1986) and location of the study valleys.

model. The model could be applied to many other valleys in this area, but that was not the purpose of this study.

### Geology

The bedrock geology of the mountains in the area ranges from Tertiary volcanic to Precambrian metamorphic rocks (Ross and others, 1955). Because the model used in this study is only dependent on the valley cross-sectional shape, and the U-shape of a glacial valley is independent of bedrock type (Graf, 1970), differences in lithology from valley to valley should not have affected the results of this study. Varying lithologies along the axis of a glacier could produce irregularities in the profile of the glacier (Flint, 1971), however, stepped valleys were not used in this study because of the problems in calculating mass flux created by extensional and compressional flow.

### Present Climate

The varied topography of the study area makes use of the traditional climatic classifications (e.g. Köppen) using mean temperature and precipitation almost impossible. Temperature and precipitation vary over short distances because of the terrain (Harding, 1982) and create a patchwork of climate types which are largely a function of elevation. However, general trends in air mass domination and moisture sources can be determined.

Mitchell (1969) classifies the climate of this region using equivalent potential temperature (the temperature that a parcel of air would attain if it were allowed to rise pseudo-adiabatically until it has lost all its moisture and then allowed to descend back to its

original pressure (Blair and Fite, 1965)) to distinguish changes in air mass domination over the western United States. Mitchell's (1969) findings show the present study area to be dominated by moist Pacific air masses in the winter (Fig. 7) and drier interior continental air masses in the summer.

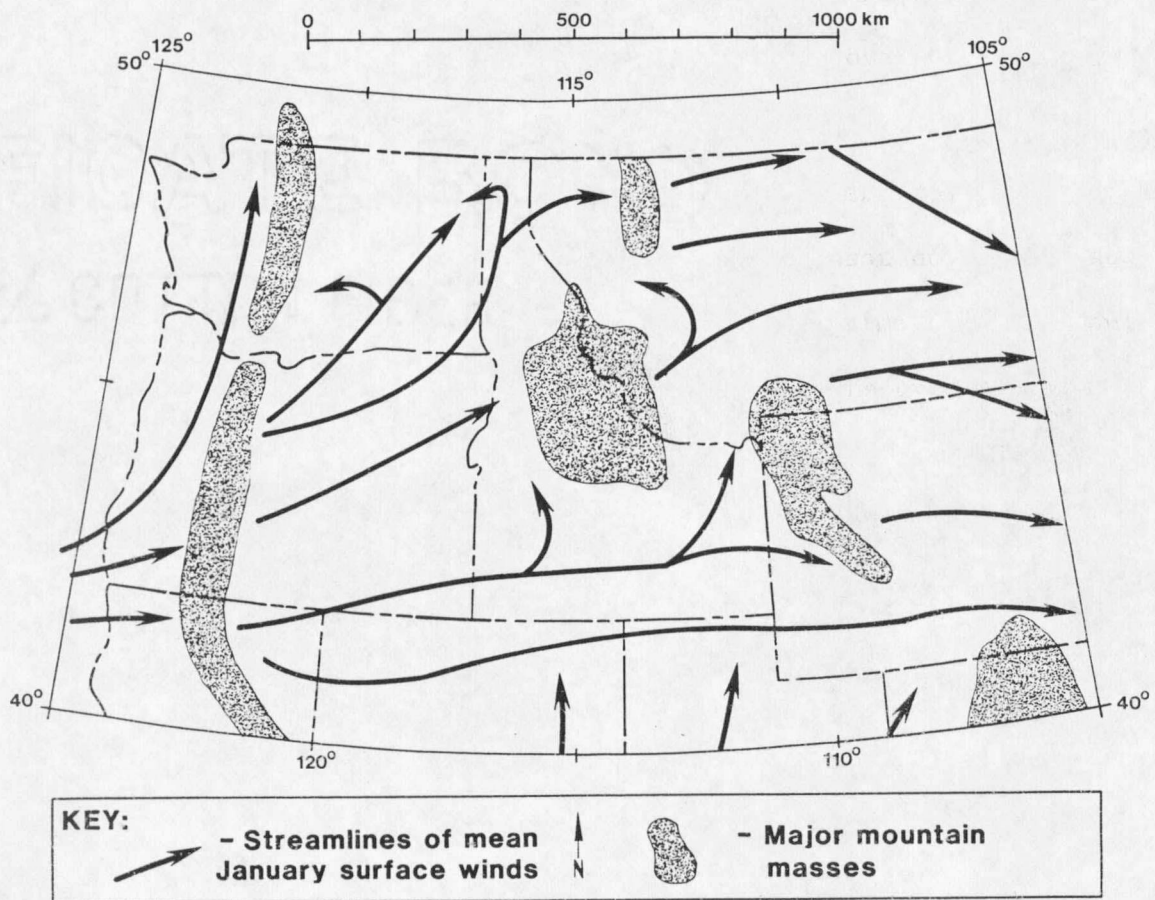


Figure 7. Streamlines of mean January surface winds over the western United States (after Mitchell, 1969).

Harding (1982) notes that the southeastern part of this study area is affected by strong upslope winds from the east during May and June accounting for precipitation maximums at this time (see Bozeman; Fig. 8). An analysis of winter precipitation patterns over western

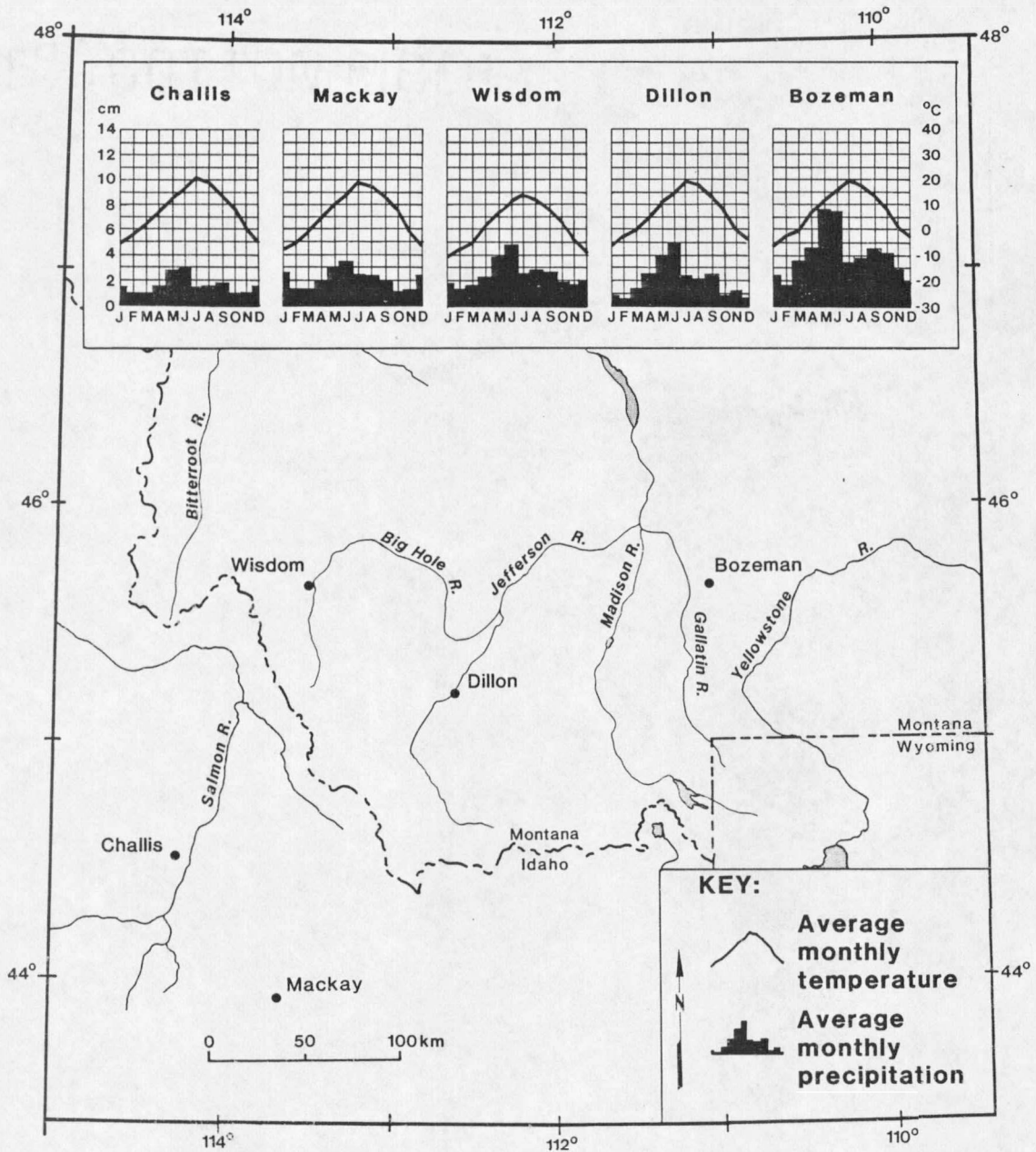


Figure 8. Climographs and locations of selected cities within the study area (data from NOAA, 1985a, 1985b).

Montana by Locke (1989) showed a dominance of Pacific moisture to the northwest with decreasing precipitation to the southeast. Locke (1989) also found a secondary source of moisture from the Gulf of Mexico into the southeastern corner of the study area, which agrees with Harding's (1982) observations.

Mountain ranges have an effect on the paths that storms follow (Price, 1981; Barry, 1981). In the study area, winter storms are steered around the central Idaho uplands allowing an influx of moisture along the Snake River Plain to the south (Fig. 7). Mackay Ranger Station, Idaho, shows a secondary maximum of precipitation in December-January (Fig. 8) which might be accounted for by its position on the northern boundary of the Snake River Plain (Fig. 5).

Mountains also affect the local, as well as regional, precipitation patterns. Precipitation usually increases with increasing elevation due to the orographic effects of mountains, thus precipitation differences occur between valleys and mountains. Bozeman, Montana (Fig. 8) has a 12 cm higher annual average precipitation than Belgrade 13 km to the west because of the orographic effects of the Bridger Range (Harding, 1982). The effect of elevation on precipitation is also noticeable in snowpack records. Plots of maximum winter snowpack versus elevation for the Lemhi, Beaverhead and Crazy Mountains are shown in Figure 9. In addition to the increase of precipitation with elevation, these gradients also show that precipitation amounts at a given elevation are lower in the western portion of the study area (Lemhi Range) and increase to the east.

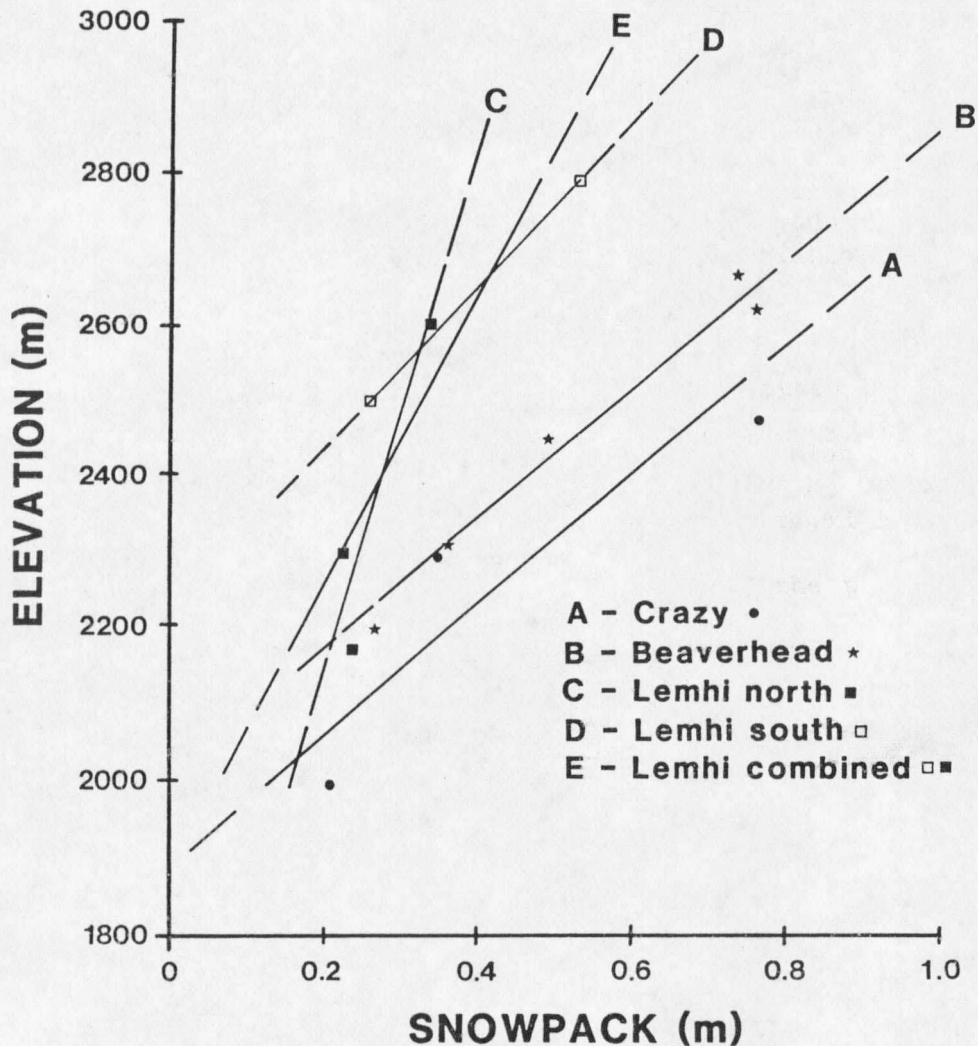


Figure 9. Modern snow accumulation gradients for the mountain ranges of the study valleys (data from Soil Conservation Service, 1986a, 1986b).

Present climates supporting alpine glaciers within the studied areas exist only in the Crazy Mountains of Montana. Glacial climates do exist outside the study area: in the Beartooth Mountains to the southeast, the Salmon River Mountains of Idaho to the west, and in several of the mountain ranges (Mission, Swan, Flathead) to the north (Field, 1975; Graf, 1976).



### Late-Pleistocene Climate

During the late Pleistocene, the Cordilleran and Laurentide ice sheets that lay to the north of the study area (Fig. 6) were up to 1500 m thick in Montana (Waitt and Thorson, 1983). The presence of this ice not only altered the topography, but probably the temperature gradients as well, which in turn, modified regional windflow and precipitation patterns (Manabe and Broccoli, 1985; Kutzbach and Wright, 1985; Locke and Kempf, 1987).

General Circulation Models (GCMs) (Kutzbach and Wright, 1985; Manabe and Broccoli, 1985) show a split jet stream over the Laurentide ice sheet over North America during the last glacial maximum. This split left most of the study area in a zone of weak westerlies with a slight easterly flow on the eastern edge. Such a wind flow pattern would suggest a Pacific moisture source for most of the area, with the possibility of a low level Gulf of Mexico source for the eastern edge. The paleoprecipitation patterns determined by Locke and Kempf (1987) show a trend of increasing moisture to the north and west over western Montana, agreeing with a dominant Pacific moisture source. Their data also suggest that the Snake River Plain and Gulf of Mexico were locally important sources of moisture.

Summer temperatures in the Northern Rocky Mountains during the last glacial maximum have been estimated to be at least 10° C lower than present (Porter and others, 1983; Barry, 1983; Kutzbach and Wright, 1985; Manabe and Broccoli, 1985). A strong temperature gradient is interpreted by the GCMs (Kutzbach and Wright, 1985; Manabe and Broccoli, 1985) along the edge of the ice sheets in the Northern

Rocky Mountains. While the paleoclimatic analysis in this study did not address climate, temperature is important in modelling the ice dynamics.

The present study provides estimates of average annual net accumulation at each glacier locality in addition to an analysis of the dynamics of each paleoglacier. While the sample size in this study is too small to provide accurate regional estimates of paleoprecipitation patterns, it does provide independent spot checks on other paleoclimatic studies in this area (Kutzbach and Wright, 1985; Manabe and Broccoli, 1985; Locke and Kempf, 1987). The results of this study are also compared with modern precipitation data for each locality.

## METHODS

This chapter details the methods, and underlying assumptions, employed in this study. These methods were tested and refined using the Big Timber Canyon paleoglacier on the east flank of the Crazy Mountains, Montana and the results from that test case are discussed in the next chapter.

A model involving glacier flow theory can be used to determine mass balance parameters using the geologic evidence left by glaciers (Fig. 1). Underlying each of the steps in this model are certain assumptions, detailed in this chapter, that affect the accuracy of the results. Figure 10 shows the flow of the methodology used in this study to reconstruct the glacier dynamics and paleoclimate. Basically, the following steps were taken during the reconstructions: 1) selection of a study valley according to specific criteria, 2) reconstruction of the glacier profile and areal extent, 3) calculation of average effective basal shear stress along the longitudinal profile, 4) calculation of mass flux from ice flow equations, 5) calculation of mass balance gradients from the calculated mass flux at the point of highest ice deformation and through the equilibrium-line altitude (ELA), and 6) climatic interpretation of the results by comparison to modern analogs. To ensure the accuracy of the results, a sensitivity analysis was performed during steps 3, 4, and 5 by varying parameters such as glacier thickness and slope (see Results).

























































































































































































































































































































